The Effect of Polyhydroxy Fullerene Derivative on Human Myeloid Leukemia K562 Cells

Meilan Yu (meilanyu@zstu.edu.cn)
Zhejiang Sci-Tech University https://orcid.org/0000-0002-5571-5332
Chan Wang
Zhejiang Sci-Tech University
Xing Liu
Zhejiang Sci-Tech University
Kollie Larwubah
Zhejiang Sci-Tech University
Wei Guo
Zhejiang Sci-Tech University
Lianjie Ye
Zhejiang Sci-Tech University Shaoxing Academy of Biomedicine
Xiangxian Ying
Zhejiang University of Technology
Jun Zhu
Hangzhou Wahaha Co., Ltd
Shengjie Yang
Hangzhou Wahaha Co., Ltd

Research Article

Keywords: Fullerenol,K562 cells,Proliferation,Apoptosis

Posted Date: April 29th, 2021

DOI: https://doi.org/10.21203/rs.3.rs-371225/v1

Abstract

The use of nanomedicines for cancer treatment has been widespread. Fullerenes have significant effects in the treatment of solid tumors. Here, we are going to study the effects of hydroxylated fullerene $C_{60}(OH)_n$(n = 18–22) treatment on chronic myeloid leukemia cell proliferation and investigates its toxicity. The results show that fullerenol at low concentrations (< 120μM) is no apparent toxic side effects and stimulates the growth of K562, while a high concentration of fullerenol has different degrees of inhibition on K562 cells. When the concentration is higher than 160μM, the K562 cells showed morphological changes, the mitochondrial membrane potential decreased, the cell cycle was blocked in the stage of G2, and cell apoptosis occurred, which may cause apoptosis, autophagy, and a variety of other damage leading to cell death. Meanwhile, it also indicated that its inhibition of solid tumors might be related to the tumor microenvironment; we verified the safety of fullerene without apparent cellular toxicity at a specific concentration.

Introduction

Fullerene, as a carbon nano-material, has received extensive attention and research since it was discovered in 1985 [1]. Due to the water insolubility of unmodified fullerenes, various physical and chemical modifications have been used to improve the primordial fullerene so that they have superb water solubility and biocompatibility [2–5]. After the modification, the unique structure and physicochemical properties (such as small size, large specific surface area, ultra-high reactivity, and functional surface modification etc.) make it has a very broad application prospect in many fields including biomedicine. As nanomaterial, fullerene derivatives have good biological safety, and have antioxidant and cytoprotective effects, antibacterial activities, antiviral effects, carrier drugs, and tumor treatment activities [6–14]. Among the diverse fullerene derivatives, polyhydroxylated fullerenes (known as fullerenols) are the most commonly used for their excellent targeting, slow-release properties, long-term effects, less dosage, and fewer adverse reactions, and so on [15]. Lajos P et al. [8] comprehensive analysis shows that $Gd@C_{82}(OH)_{22}$ NPs maintain their remarkable anti-cancer effect in a variety of solid tumors. Chunying Shu et al. [16] chose luciferase-expressing mouse breast cancer cell line 4T1-luc as the xenograft model, they found after light irradiation, the activated Gd-Ala could make full use of oxygen in blood vessels to produce ROS resulting in partial or complete vascular disruption. These results obtained clarify that fullerene derivative nanomaterials are potential candidates for cancer drugs with high efficacy and low toxicity [8, 17], which may open a new perspective for biomedicine. As for the research on whether nanoparticles can be used as new and highly effective anti-malignant chemotherapeutics, Chunru Wang et al. [5] synthesized water-soluble fullerenes C_{70}-Lys and C_{70}-Ala, it demonstrated the superiority of C_{70}-Lys compared with C_{70}-Ala against the chemotherapy injuries that induced by doxorubicin, further experiments in mice with hepatotoxicity and cardiotoxicity models also confirmed it. Many scientists like Yuliang Zhao et al. [18] believe that the anti-tumor effect of fullerenes is mainly through changing the tumor microenvironment, Mingming Zhen et al. [19] demonstrated GF-Ala nanoparticles reprogram TAMs from tumor promoting M2 phenotype to tumoricidal M1 phenotype and

increase the infiltration of cytotoxic T lymphocytes, rebuilding immunosuppressive tumor microenvironment and achieving positively effective inhibition of tumor growth. Zhiyi Chen [20] found that in the acidic tumor microenvironment, the hydrophobic-to-hydrophilic conversion of the pH-responsive polymer DOX-RNPs leads to drug release simultaneously and no noticeable histological changes were observed in major organs of mice treated with RNPs. Therefore, it is necessary to study the biological characteristics and clinical application of polyhydroxy-fullerenols in biomedicine, especially in malignant tumors and non-solid tumors.

The most common non-solid tumor is known as leukemia, leukemia is a clonal malignant disease with abnormal hematopoietic stem cells [21]. According to the acute illness and the maturity of leukemia cells, it can be divided into acute and chronic leukemias according to the type of proliferating cells, it can be divided into lymphocytic leukemia and myeloid leukemia. Chemotherapy is currently the mainstream for clinical Leukemia treatments. Chronic myeloid leukemia (CML) is a kind of hematological malignancy characterized by the expression of oncogenic kinase BCR-ABL. K562 cells were isolated from the pleural fluid of a female patient with acute chronic myeloid leukemia. The K562 protocell is a malignant hematopoietic cell with multiple differentiation potential, which is a highly sensitive target to natural killer cells in vitro and is widely used in this convenient study, so we chose the K562 cell as non-solid tumors research target. A Profound change has taken place in the therapy of chronic myeloid leukemia (CML) over the past several years. In western countries, the median age of CML patients is about 57 years, more than 20% of patients are over 70 years old and children and adolescents are < 5% [22], while in Asia and Africa the median age at diagnosis is < 50 years [23]. Comparing with other tumors, the harm to humans is more obvious and prominent. Finding high-efficiency and low-toxicity leukemia treatment drugs is an urgent problem to be solved [24].

However, throughout these studies on the effect of fullerenes on cancer, most of them about the effect of fullerenes is solid tumors [16, 19], there is little research on the specific non-solid tumor cancer-blood cancer. In particular, there are few studies have been reported the anticancer activity of $C_{60}(OH)_n$(n = 18–22) in vitro on the chronic myeloid leukemia cell line K562 cells. To investigate the proliferation and toxicity of fullerenes on myeloid leukemia cells will not only help to explore the mechanism of blood malignant tumor suppression but also may provide more references and options for further development of fullerenol as a target to non-tumor therapeutic.

Materials And Methods

Materials

Water-soluble polyhydroxy fullerenol $C_{60}(OH)_n$ (n=18-22) was synthesized in an aqueous phase by Xiamen Funaxin Materials Technology Co., Ltd. The RPMI-1640 medium was purchased from Gibco Co., Ltd. The fetal bovine serum was purchased from Zhejiang Sijiqing Biotechnology Co., Ltd, China. Dimethyl sulfoxide (DMSO) was obtained from Sigma Company. Doxorubicin hydrochloride was purchased from Shanghai McLean biochemical technology Co., Ltd. AO/EB staining kit was supplied by

Solarbio, Inc. Cell Counting kit-8 was purchased from Tongren Institute of Chemistry, Japan. Trypan blue was obtained from GE Healthcare Co., Ltd. Cell Cycle Detection Kit, Apoptosis Detection Kit, and Jc-1 Cell apoptosis Mitochondrial membrane potential Detection Kits were purchased from Nanjing Kaiji Biotechnology Development Co., Ltd. The other reagents were analytically pure. Experiments with water are ultrapure water (Double - distilled water, 18.2 MΩ, cm). The chemicals and solvents were purchased from commercial sources.it is analytical grade and used without further purification unless otherwise stated.

Human chronic myelocytic leukemia cell line K562 derived from Institutes of Biological Sciences, Chinese Academy of Sciences, Shanghai, China.

Cell proliferation inhibition assay

Leukemia cells K562 and normal liver cells L-02 in the logarithmic phase were inoculated with a density of 4×10^4/mL on a 96-well culture plate. The control group was added with the same amounts of cells and a complete medium of RPMI-1640. Fullerenol $C_{60}(OH)_n$ (n=18-22) diluted with RPMI-1640 culture medium was added to the treatment group to obtain final concentrations of 40, 60, 80, 100, 120, 160, 240, and 320μmol/L, respectively. Adriamycin was used as the positive control group and blank holes were set. Six multiple wells were set for each well, the A_{450} values of each well at 24 and 48 hours were determined by enzyme-linked immunoassay (Thermo, USA), and the inhibition rate of cell proliferation was calculated according to the following formula:

Proliferation inhibition rate = $(A_{control} - A_{administration}) / (A_{control} - A_{blank}) \times 100\%$

Cell cycle assay

K562 cells in the logarithmic phase were adjusted to the concentration of 1.5×10^5/mL, and the cells were inoculated into a 6-well culture plate, 2 mL of cell fluid was added into each well, the experimental group immediately added $C_{60}(OH)_n$ (n-18-22) with the final concentration of 0, 40, 60, 80, 100, 120, 160, 240 and 320μmol/L, respectively. The control added the same amounts of cells and complete medium of RPMI1640. The cells were cultured at 37°C and 5% CO_2 for 48 hours and then collected. Pre-cooled PBS was rinsed 2 times, and the cells were resuspended in the pre-cooled 75% ethanol for more than 24 hours at -20°C. Before staining, it was washed with PBS and the cell density was adjusted to 1×10^6/mL. Then the cells were collected in the flow tube, added 100μL of RNase A, bathed in the water at 37°C for 30 min, then add 400μL PI staining solution, slowly and fully resuspended cells. The cells were incubated at 4°C in dark for 30 min, filtered with 400 nylon membranes, then placed in an ice bath and flow cytometry (BD, USA) was used to detect the red fluorescence and light scattering at the excitation wavelength of 488 nm, the changes of the cell cycle were analyzed. The experiment was repeated three times, and the cell proliferation index was calculated according to the formula:

PI= (S+G2/M)/(G0/G1+S+G2/M)

Cell morphology assay

The growth inhibition effect of different concentrations of $C_{60}(OH)_n$(n=18-22) on human leukemia cell line K562 in vitro for 48h was observed by light microscopy. K562 cells were inoculated in a 96-well plate at a concentration of 1×10^4/well, treated with $C_{60}(OH)_n$ at different doses for 48h, then using fluorescence microscope observation and photography, the growth inhibition of K562 cells by $C_{60}(OH)_n$ was observed.

Detection of apoptosis

The grouping and dosing status of the K562 cells were the same as that of 2.5. The blank control group and the monochrome control group were set and cultured at 37℃ and 5% CO_2 for 48 hours. About 1×10^6 cells were collected by centrifugation and washed with precooled PBS for 2 times, PBS was discarded and 100μL binding buffer was added to make a single-cell suspension. Before staining, the cells were filtered with a 400-mesh sieve for 2 times, Annexin v-FITC 5μL and PI 5μL were added in turn, after mixing stained in the dark at 4℃ for 30 min, the apoptosis rate of each group was detected by flow cytometry within 1 hour after 400μL binding buffer was added and the experiment was repeated three times.

Induction of apoptosis and AO/EB double staining

After the cells reached 80% confluence, $C_{60}(OH)_n$ was added for 48 hours, the single-cell suspension was prepared. The cell concentration was adjusted to 10^6/mL with PBS, 25μL cell suspension was taken, then the cells were treated with 2μL of AO (100μg/mL) and 2μL EB (100μg/mL), beat and mix, drop on the slide, cover and seal the slide, and observe the morphology of apoptotic cells by fluorescence microscope.

Analysis of mitochondrial membrane potential

The cell suspension was washed with JC-1 staining buffer solution for 2 times, the cell concentration was adjusted to 1×10^6/mL, 0.5 mL of JC-1 staining solution with a final concentration of 10μg/mL was added, and the mixture was then placed in a CO_2 incubator for further incubation in the dark for 20 min. Centrifuge with 900×g for 6 min, discard supernatant, wash with JC-1 staining buffer solution twice, centrifuged with 900×g for 6 min every time. Discard the supernatants and add 500μL JC-1 stain buffer per tube. The cells were detected by flow cytometry, the detection data obtained and analyzed by Cell Quest functional software. The excitation wavelength was 488 nm, and 10,000 cells were collected for each sample.

Electron microscopy of cell apoptosis

K562 cells in the logarithmic growth stage were inoculated in a 6-well culture plate with 1.5×10^8/L, and different concentrations of $C_{60}(OH)_n$ were added for intervention. The control group was supplemented with an equal volume of serum-containing medium without drugs. After culturing for 48 h, 800 r/min was centrifuged for 10 min. The culture medium was discarded and 2.5% glutaraldehyde was added to fix it for 2h. Samples were prepared according to the requirements of the transmission electron microscope experiment, including embedding, polymerization, and ultra-thin slicing machine. After double staining with lead citrate, the ultrastructural characteristics of the cells were observed under the electron microscope.

Data analysis

All experiments were repeated independently at least three times and all data presented are means or means ± standard deviations. Statistical analysis was carried out by analysis of variance (ANOVA) followed by appropriate post hoc tests including multiple comparison tests (LSD). All analyses were made using SPSS 11.5 statistical software package and $P<0.05$ were recognized as statistically significant (*) and $P < 0.01$ were greatly statistically significant (**).

Results

Effects of $C_{60}(OH)_n$ on the proliferation of K562 cells

The effects of $C_{60}(OH)_n$ on cell proliferation are shown in Fig. 1 and Fig. 2. The cells were cultured in a medium containing $C_{60}(OH)_n$ for 24 hours, it was no obvious regular change in cell proliferation, while the cells were cultured in a medium containing $C_{60}(OH)_n$ for 48 hours and at certain concentrations, the inhibitory effect of $C_{60}(OH)_n$ on proliferation began to appear and was relatively stable (Fig. 2).That is, when the concentration of $C_{60}(OH)_n$ is lower than 120μmol/L, it can promote the proliferation of K562 cells and cell inhibition began to appear when the concentration was above 160μmol/L. $C_{60}(OH)_n$ can inhibit the growth of K562 cells significantly, and the growth inhibition rate up to 40.7% when it is 320μmol/L. The results were similar with Chunying Chen [12] who proved that after incubation of cells with $C_{60}(OH)_{20}$ for 48 h, no significant influence on the cell viability of MCF-7 was observed at concentrations of 1, 10, and 100 μg/mL. With the increase of $C_{60}(OH)_n$ dose and prolonged action time, the inhibitory effect of $C_{60}(OH)_n$ is more obvious, which is $C_{60}(OH)_n$ has a certain time-dose dependent effect on K562 cell proliferation. Besides, the effect of $C_{60}(OH)_n$ on the proliferation of L-02 was studied using normal human liver cells L-02 and drug intervention as controls. The results showed that L-02 cells treated with $C_{60}(OH)_n$ did not show proliferation inhibitory activity, but instead promoted cell growth. Fig 1B confirms that the cell growth rate of the drug-treated group is significantly lower than that of the

control group when the concentration was above 160μmol/L. $C_{60}(OH)_n$ promotes cell proliferation at low concentration and inhibits its growth or induces death at high concentrations with a time-dose effect.

Effects of $C_{60}(OH)_n$ on the cell cycle of K562

The cell cycle of K562 cells was affected by a high concentration of $C_{60}(OH)_n$. It changed the ratio of S and G2-M phase cells. The S-phase cells were significantly reduced under the concentrations of 240,320μmol/L, the proportion of G2-M cells increased significantly, and the cell cycle stagnated at G2/M, with statistically significant differences ($P<0.05$). When the drug concentrations add to 640μmol/L (it's not shown here), there was no significant change in the period, and the difference was not statistically significant ($P>0.05$). It indicated increasing concentration did not influence the cell cycle (Fig. 3).

Morphological study of $C_{60}(OH)_n$ on K562 cells

K562 cells are human chronic myelogenous leukemia cell line, in general, the cells are large, usually round or oval nucleus, a large proportion of nucleus and plasma, no particles in the cytoplasm, often aggregation and growth [25]. However, when the cells were cultured in a medium containing different dose concentrations of $C_{60}(OH)_n$ for 48 hours, the number of cells increased firstly and then decreased. The cells treated with 40μmol/L-120 μmol/L $C_{60}(OH)_n$ showed little difference in morphology from the control cells. With the concentration rising above 120μmol/L, the cells begin to change, when the concentration increased to 160μmol/L, the cell size was deformed, the connections between the cells disappeared, and the cell separated from the surrounding cells. The particles in the cytoplasm increased and thickened, and the membrane was bubbled. The number of cells floating by cell lysis also increased, and the cell morphology became more irregular. With the increase of $C_{60}(OH)_n$ dose, the more obvious influences on cells, and the changes in cell morphology are more prominent. When the concentration increased to 240μmol/L and 320μmol/L, more cells floated, and the number of cells was significantly reduced compared with that of other treatment groups, indicating that there was not only a significant inhibitory effect on cell proliferation but also a large number of cell death (as shown in Fig. 4). The results were consistent with the CCK-8 proliferation assay (Fig. 1).

Effect of $C_{60}(OH)_n$ on apoptosis of K562 cells

Because of the greater inhibition effect of fullerene on K562 cells at the concentrations of 240μmol/L and 320μmol/L, the two concentrations were selected for further investigation. The apoptotic K562 cells rate was analyzed by using Annexin V-fluorescein isothiocyanate (FITC)/propidium iodide staining and flow cytometry after the action of different concentrations of fullerenol on leukemia cells for 48 h. Annexin V is a phospholipid-binding protein that exhibits a high affinity for phosphatidylserine during exposure to the extracellular environment at the early stage of apoptotic. Comparing with other detection methods based

on nuclear changes, the early stages of apoptosis can be identified more effectively. Annexin V staining represents a loss of membrane integrity, which can also occur in the anaphase of cell death. Therefore, Annexin V-FITC/PI staining is often used to identify the integrity of cell membranes, and a combination of positive/negative signals was used to differentiate early or late apoptosis and necrosis [26]. As shown in Fig. 5, $C_{60}(OH)_n$ (n=18-22) could accelerate both early apoptosis and late apoptosis in K562 cells, the 320μmol/L group was more obvious than 240μmol/L group. It was also found that the proportion of apoptotic cells increased significantly after the treatment of high concentration of $C_{60}(OH)_n$ (240, 320μM) for 48h compared with the negative control group ($P<0.05$). These results are consistent with the morphological experiments.

No apoptotic cells were observed under a fluorescence microscope in the normal control group. Early apoptotic cells were observed in the 240μmol/L group after 48h $C_{60}(OH)_n$ (n=18-22) treatment. Specifically, after AO/EB staining, the nuclei were observed to be yellow-green fluorescent, granular, and clustered on one side of the cell, showing the budding of the cell. The number of early apoptotic cells and the number of late apoptotic cells were positively correlated with the concentration. The latter is characterized by nuclear concentration and migration, and apoptotic bodies are seen (Fig. 6), apoptotic bodies are one of the important markers of cell apoptosis [27].

Effects of $C_{60}(OH)_n$ on mitochondrial membrane potential in K562 cells

The changes of mitochondrial membrane potential in leukemia K562 cells treated with $C_{60}(OH)_n$ were analyzed by multi-parameter flow cytometry using the fluorescent probe JC-1. In the process of cell apoptosis, the mitochondrial membrane structure of the cell is damaged, the membrane potential reduced and the concentration is low, and JC-1 cannot be concentrated in the mitochondrial matrix, mainly in the form of a monomer, so the red fluorescence intensity produced by the apoptotic cells is reduced. When excited at 488 nm, the maximum emission wavelength was 527 nm, showing green fluorescence, which was detected by FL1. When the membrane potential is high, the concentration is high, and aggregation is formed. When the 488 excitation occurs, the maximum emission wavelength is 590 nm, showing red fluorescence, FL2 was used for detection, and FL2 was used for the scatter plot of FL1.

As shown in Fig. 7, cells in the control group had higher activity and higher mitochondrial membrane potential. The concentration of JC-1 aggregates in mitochondria was high, and the red fluorescence was strong. The cells were concentrated in the first quadrant, and the cells in the fourth quadrant were few, accounting for only 2.82%. In 240 and 320μmol/L treated cells, the number of cells in the fourth quadrant increased gradually, accounting for 12.65% and 15.31% of the total number of cells, respectively. These results suggested that the increased dose of $C_{60}(OH)_n$ (n=18-22) caused a large number of cell apoptosis. In the fourth quadrant, the cell red light decreased, in which the concentration of JC-1 aggregation decreased. This was due to the apoptosis induced by $C_{60}(OH)_n$, resulting in the decline of mitochondrial

membrane potential, and the concentration of JC-1 in mitochondria decreased accordingly. This indicated that $C_{60}(OH)_n$ induced apoptosis through the signal transduction pathway of mitochondrial cell apoptosis.

Ultrastructural changes of cell apoptosis

The general characteristics of the ultrastructure of leukemia K562 cells were observed under transmission electron microscopy: large cell size, clear intercellular space, weak connection, intact cell membrane and nuclear membrane, double layer unit membrane, few organelles, complete mitochondrial ridge, and abundant mitochondria. There are large amounts of endoplasmic reticulum in the cytoplasm, mitochondria and rough endoplasmic reticulum are irregular and disorganized. With the increase of $C_{60}(OH)_n$ (n=18-22) concentration, the apoptotic K562 cells gradually increased and became more obvious. Some of the cells showed typical apoptotic cell morphological changes: the morphology became irregular, the cytoplasmic hollow vesicles increased, the chromatin in the nucleus agglutination, edge aggregation, etc. In the control group of 320μmol/L drugs, the proportion of cytoplasmic concentration increased, the nuclear membrane broke and disappeared, the chromatin was dispersed into several small pieces, and the chromatin such as mitochondria was solid and shrunk. The nucleus is fragmented, but the cell membrane is intact and apoptotic bodies are visible (Fig. 8).

It was seen that high dose of $C_{60}(OH)_n$ induce the K562 cell death in a certain way and the characteristic morphological changes were observed by transmission electron microscopy, that is, the proportion of nucleoplasm increased, and the nuclear material was dense, patchy, or gathered in the nuclear membrane in a crescent shape, appeared the apoptotic bodies.

Discussion

Fullerenol has no distinct toxic-side effects and $C_{60}(OH)_n$(n=18-22) promoted proliferation in low concentrations(<120μmol/L), while high concentrations(160-320μmol/L) fullerenol inhibited cell proliferation and leading to cell apoptosis. We further explored the Morphological change and ultrastructural characteristics of K562 cells, obvious morphological changes and the appearance of apoptotic bodies were observed. It can block K562 cells in the stage of G2, making mitochondrial membrane potential decline and inducing cell apoptosis. These results supported that high concentration fullerenol $C_{60}(OH)_n$ leading to chronic myeloid leukemia K562 cells apoptotic and showed a good dose-effect relationship. However, there was no cytotoxicity or damage to L-02 and K562 cells at low concentrations and even promoted its proliferation. At the same time, this phenomenon is consistent with lots of researches that fullerenes have no toxic side effects.

In the present study, we found that the mitochondrial membrane potential level of the fullerenol treatment group was significantly reduced, indicating that the K562 cell death, may be related to the signal transduction pathway of cell apoptosis induced by mitochondria. The mechanism of high concentration

fullerenol inhibiting the proliferation and inducing apoptosis of K562 cells may involve a complex process of multiple signal transduction pathways, and apoptosis may also be one of the mechanisms of its anti-tumor effect. In conclusion, fullerenols of high concentration may cause cell death in various ways including apoptosis, autophagy, and macromolecule formation, which may be caused by a series of damage caused by high concentration, rather than the inhibitory effect of the drug itself on K562 cells. Besides, fullerenol contains -OH, in high concentrations, which may form hydrogen bonds and further form macromolecules that adhere to the surrounding cells, so that they can't get nutrients, respiration is affected, thus causing cell damage and death. The involvement of specific molecular mechanisms is still unknown, which needs further study.

Current cancer treatments mainly including change the microenvironment, anti-angiogenesis, drug resistance, improve immunity, mediated chemical sensitization, and so on, but most of the fullerenols antitumor research has focused on breast cancer, lung cancer, and other solid tumors. Leukemia as a non-solid tumor, the change of the internal environment is not to control. Thus, the synergistic effect of fullerenol and commonly used chemoradiotherapy drugs can be considered for solid tumors, which can not only inhibit tumors but also reduce the toxicity and side effects brought by chemoradiotherapy. The use of antioxidants as co-adjuvant therapy can reduce the toxic and side effects of pro-oxidant drugs, while antioxidants can reduce the cytotoxicity of many drugs. Although our experimental results don't show a well therapeutic effect of $C_{60}(OH)_n$ for chronic myeloid leukemia of K562 cells. In future studies, we can try to change the number of hydroxyl groups, add amino acids or functional modification functions on fullerenols to explore their influence on leukemia cells and animal research. It can also provide a basis for further research on the therapeutic effects of fullerene derivatives on non-solid tumor like leukemia.

Declarations

Data availability

The data sets used and analyzed that support the findings of this study are available from the corresponding author upon reasonable request.

Author Contributions

CW, XL and MLY conceived and designed the study, CW and XL performed most of the experimental procedures and wrote the manuscript. KL, WG and LJY performed experiments and/or analyzed the resulting data. XXY and SJY provided the laboratory resources, JZ helped in analysing the data.

Acknowledgments

The project was supported by Open Fund of Shaoxing Academy of Biomedicine of Zhejiang Sci-Tech University. The project was supported by Zhejiang University of Technology Research Stare-up Fund (No:15042089-Y).

Compliance with ethical standards

This article does not contain any studies with human participants or animals performed by any of the authors.

Conflict of interest

The authors confirm that there is no conflict of interest.

References

1. H.W.Kroto (1985) C_{60}Buckminsterfullerene.
2. LAURA L. DUGAN*† DMT (1997) Carboxyfullerenes as neuroprotective agents.
3. Xiao L, Hong K, Roberson C, Ding M, Fernandez A, Shen F, Jin L, Sonkusare S and Li X (2018) Hydroxylated Fullerene: A Stellar Nanomedicine to Treat Lumbar Radiculopathy via Antagonizing TNF-alpha-Induced Ion Channel Activation, Calcium Signaling, and Neuropeptide Production. ACS Biomater Sci Eng 4:266-277. doi: 10.1021/acsbiomaterials.7b00735
4. Li J, Guan M, Wang T, Zhen M, Zhao F, Shu C and Wang C (2016) Gd@C_{82}-(ethylenediamine)$_8$ Nanoparticle: A New High-Efficiency Water-Soluble ROS Scavenger. ACS Appl Mater Interfaces 8:25770-25776. doi: 10.1021/acsami.6b08659
5. Zhou Y, Zhen M, Guan M, Yu T, Ma L, Li W, Zheng J, Shu C and Wang C (2018) Amino acid modified [70] fullerene derivatives with high radical scavenging activity as promising bodyguards for chemotherapy protection. Sci Rep 8:16573. doi: 10.1038/s41598-018-34967-7
6. Huan Meng GX, Baoyun Sun, Feng Zhao (2010) Potent Angiogenesis Inhibition by the Particulate Form ofFullerene Derivatives.
7. Zhu J, Ji Z, Wang J, Sun R, Zhang X, Gao Y, Sun H, Liu Y, Wang Z, Li A, Ma J, Wang T, Jia G and Gu Y (2008) Tumor-inhibitory effect and immunomodulatory activity of fullerol $C_{60}(OH)_x$. Small 4:1168-75. doi: 10.1002/smll.200701219
8. Balogh LP (2015) Caging cancer. Nanomedicine 11:867-9. doi: 10.1016/j.nano.2015.02.005
9. Ya-Wen Chen KCH, Cheng-Chieh Yen (2004) Fullerene derivatives protect against oxidative stress in RAW 264.7 cells and ischemia-reperfused lungs.
10. Nakagawa Y, Suzuki T, Ishii H, Nakae D and Ogata A (2011) Cytotoxic effects of hydroxylated fullerenes on isolated rat hepatocytes via mitochondrial dysfunction. Arch Toxicol 85:1429-40. doi: 10.1007/s00204-011-0688-z

11. Markman JL, Rekechenetskiy A, Holler E and Ljubimova JY (2013) Nanomedicine therapeutic approaches to overcome cancer drug resistance. Adv Drug Deliv Rev 65:1866-79. doi: 10.1016/j.addr.2013.09.019
12. Jiao F, Liu Y, Qu Y, Li W, Zhou G, Ge C, Li Y, Sun B and Chen C (2010) Studies on anti-tumor and antimetastatic activities of fullerenol in a mouse breast cancer model. Carbon 48:2231-2243. doi: 10.1016/j.carbon.2010.02.032
13. Ueno H, Yamakura S, Arastoo RS, Oshima T and Kokubo K (2014) Systematic Evaluation and Mechanistic Investigation of Antioxidant Activity of Fullerenols Usingβ-Carotene Bleaching Assay. Journal of Nanomaterials 2014:1-7. doi: 10.1155/2014/802596
14. Semenov KN, Charykov NA, Postnov VN, Sharoyko VV, Vorotyntsev IV, Galagudza MM and Murin IV (2016) Fullerenols: Physicochemical properties and applications. Progress in Solid State Chemistry 44:59-74. doi: 10.1016/j.progsolidstchem.2016.04.002
15. Zhou Y, Zhen M, Ma H, Li J, Shu C and Wang C (2018) Inhalable gadofullerenol/[70] fullerenol as high-efficiency ROS scavengers for pulmonary fibrosis therapy. Nanomedicine 14:1361-1369. doi: 10.1016/j.nano.2018.03.008
16. Guan M, Zhou Y, Liu S, Chen D, Ge J, Deng R, Li X, Yu T, Xu H, Sun D, Zhao J, Zou T, Wang C and Shu C (2019) Photo-triggered gadofullerene: enhanced cancer therapy by combining tumor vascular disruption and stimulation of anti-tumor immune responses. Biomaterials 213:119218. doi: 10.1016/j.biomaterials.2019.05.029
17. Meng J, Liang X, Chen X and Zhao Y (2013) Biological characterizations of $[Gd@C_{82}(OH)_{22}]_n$ nanoparticles as fullerene derivatives for cancer therapy. Integr Biol (Camb) 5:43-7. doi: 10.1039/c2ib20145c
18. Liu Y, Chen C, Qian P, Lu X, Sun B, Zhang X, Wang L, Gao X, Li H, Chen Z, Tang J, Zhang W, Dong J, Bai R, Lobie PE, Wu Q, Liu S, Zhang H, Zhao F, Wicha MS, Zhu T and Zhao Y (2015) Gd-metallofullerenol nanomaterial as non-toxic breast cancer stem cell-specific inhibitor. Nat Commun 6:5988. doi: 10.1038/ncomms6988
19. Li L, Zhen M, Wang H, Sun Z, Jia W, Zhao Z, Zhou C, Liu S, Wang C and Bai C (2020) Functional Gadofullerene Nanoparticles Trigger Robust Cancer Immunotherapy Based on Rebuilding an Immunosuppressive Tumor Microenvironment. Nano Lett 20:4487-4496. doi: 10.1021/acs.nanolett.0c01287
20. Wang S, Zhou Z, Wang Z, Liu Y, Jacobson O, Shen Z, Fu X, Chen ZY and Chen X (2019) Gadolinium Metallofullerene-Based Activatable Contrast Agent for Tumor Signal Amplification and Monitoring of Drug Release. Small 15:e1900691. doi: 10.1002/smll.201900691
21. C HARLES L. S AWYERS MD (1999) CHRONIC MYELOID LEUKEMIA.
22. Hochhaus A, Baccarani M, Silver RT, Schiffer C, Apperley JF, Cervantes F, Clark RE, Cortes JE, Deininger MW, Guilhot F, Hjorth-Hansen H, Hughes TP, Janssen J, Kantarjian HM, Kim DW, Larson RA, Lipton JH, Mahon FX, Mayer J, Nicolini F, Niederwieser D, Pane F, Radich JP, Rea D, Richter J, Rosti G, Rousselot P, Saglio G, Saussele S, Soverini S, Steegmann JL, Turkina A, Zaritskey A and Hehlmann R

(2020) European LeukemiaNet 2020 recommendations for treating chronic myeloid leukemia. Leukemia 34:966-984. doi: 10.1038/s41375-020-0776-2

23. Hemant Malhotra JR, and Pat Garcia-Gonzalez (2019) Meeting the needs of CML patients in resource-poor countries.
24. Liu WJ, Zhang T, Guo QL, Liu CY and Bai YQ (2016) Effect of ATRA on the expression of HOXA5 gene in K562 cells and its relationship with cell cycle and apoptosis. Mol Med Rep 13:4221-8. doi: 10.3892/mmr.2016.5086
25. Eva KLEIN HB-B (1976) PROPERTIES OF THE K562 CELL LINE, DERIVED FROM A PATIENT WITH CHRONIC MYELOID LEUKEMIA.
26. Lee CW, Chi MC, Peng KT, Chiang YC, Hsu LF, Yan YL, Li HY, Chen MC, Lee IT and Lai CH (2019) Water-Soluble Fullerenol $C_{60}(OH)_{36}$ toward Effective Anti-Air Pollution Induced by Urban Particulate Matter in HaCaT Cell. Int J Mol Sci 20. doi: 10.3390/ijms20174259
27. Yamamoto TIT (1998) The process of ultrastructural changes from nuclei to apoptotic body.

Figures

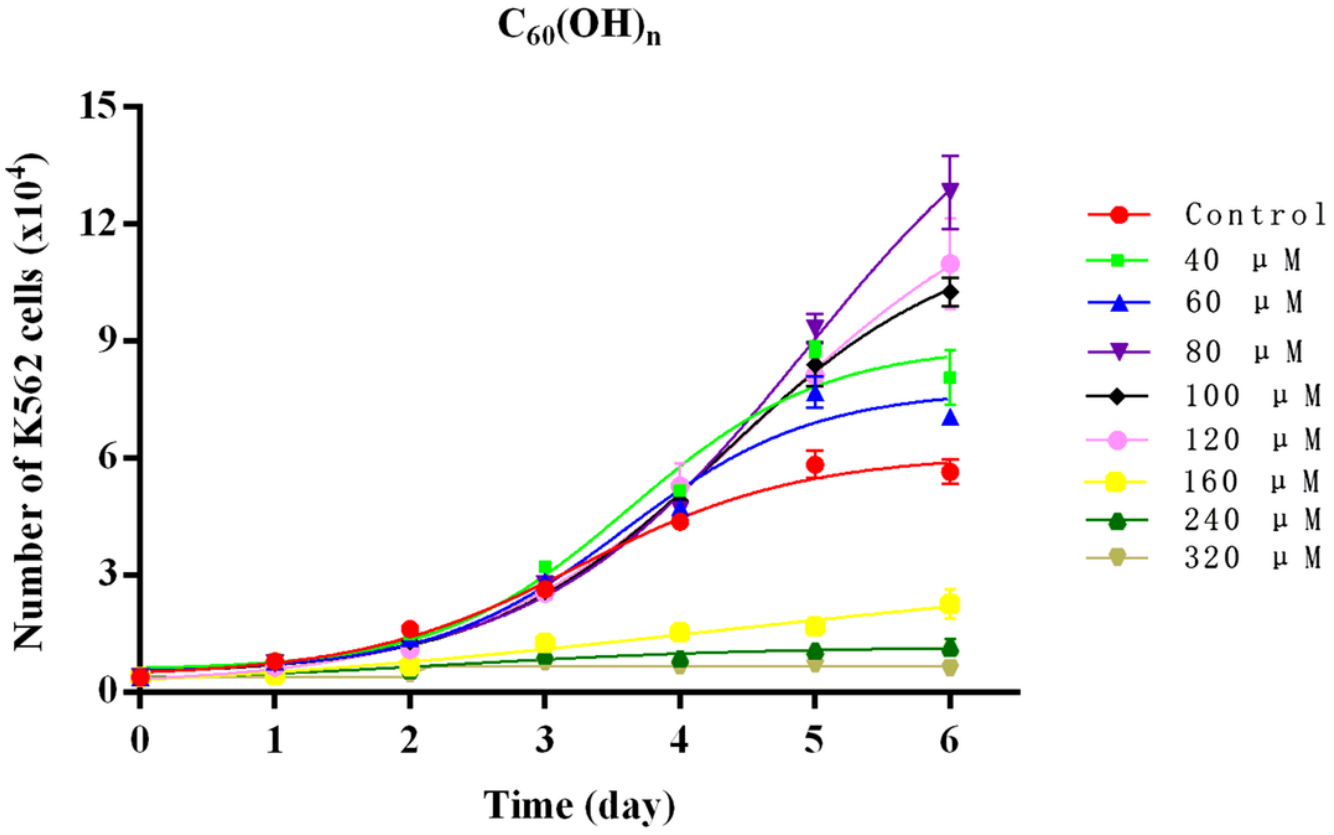

Figure 1

The growth curve method showed the C60(OH)n had a dose and time-effect effect on the proliferation of cell K562.

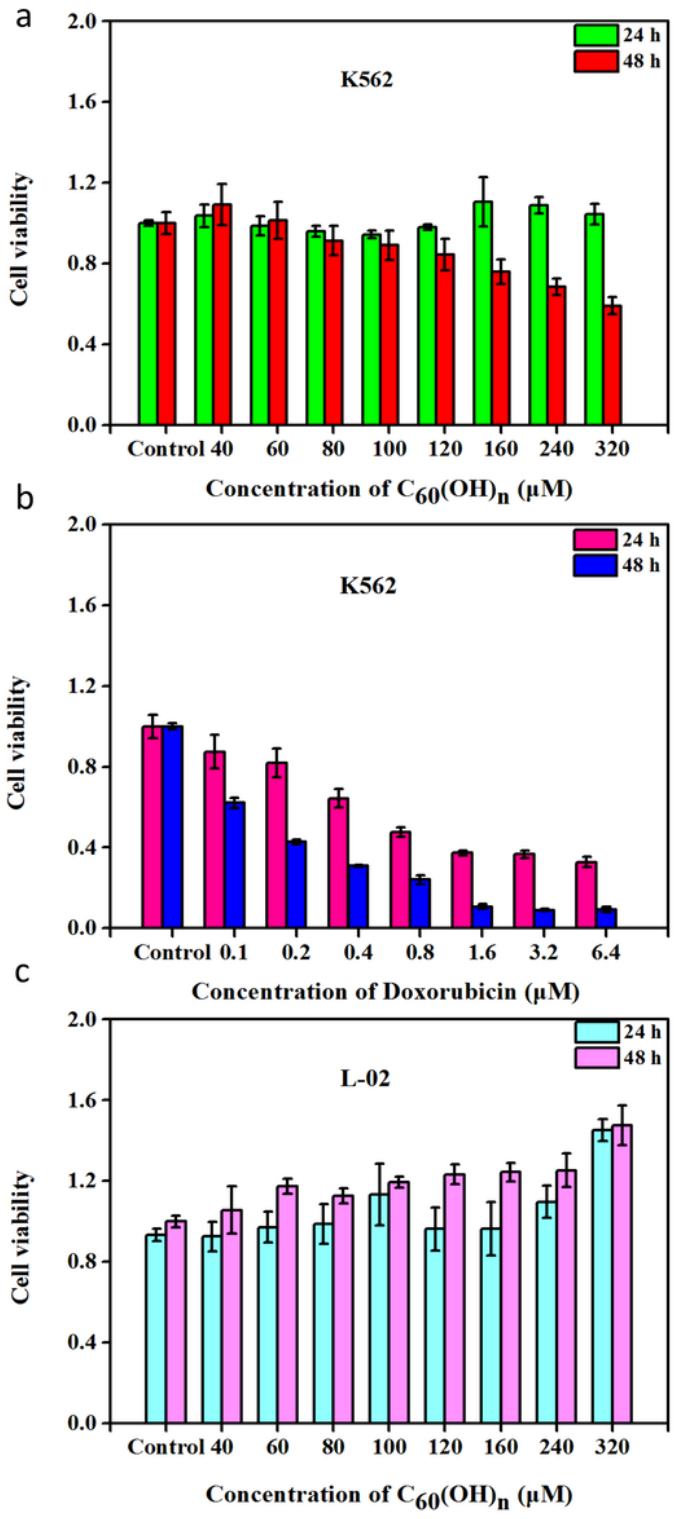

Figure 2

The growth-inhibitory effects of C60(OH)n and Doxorubicin on human myeloid leukemia. K562

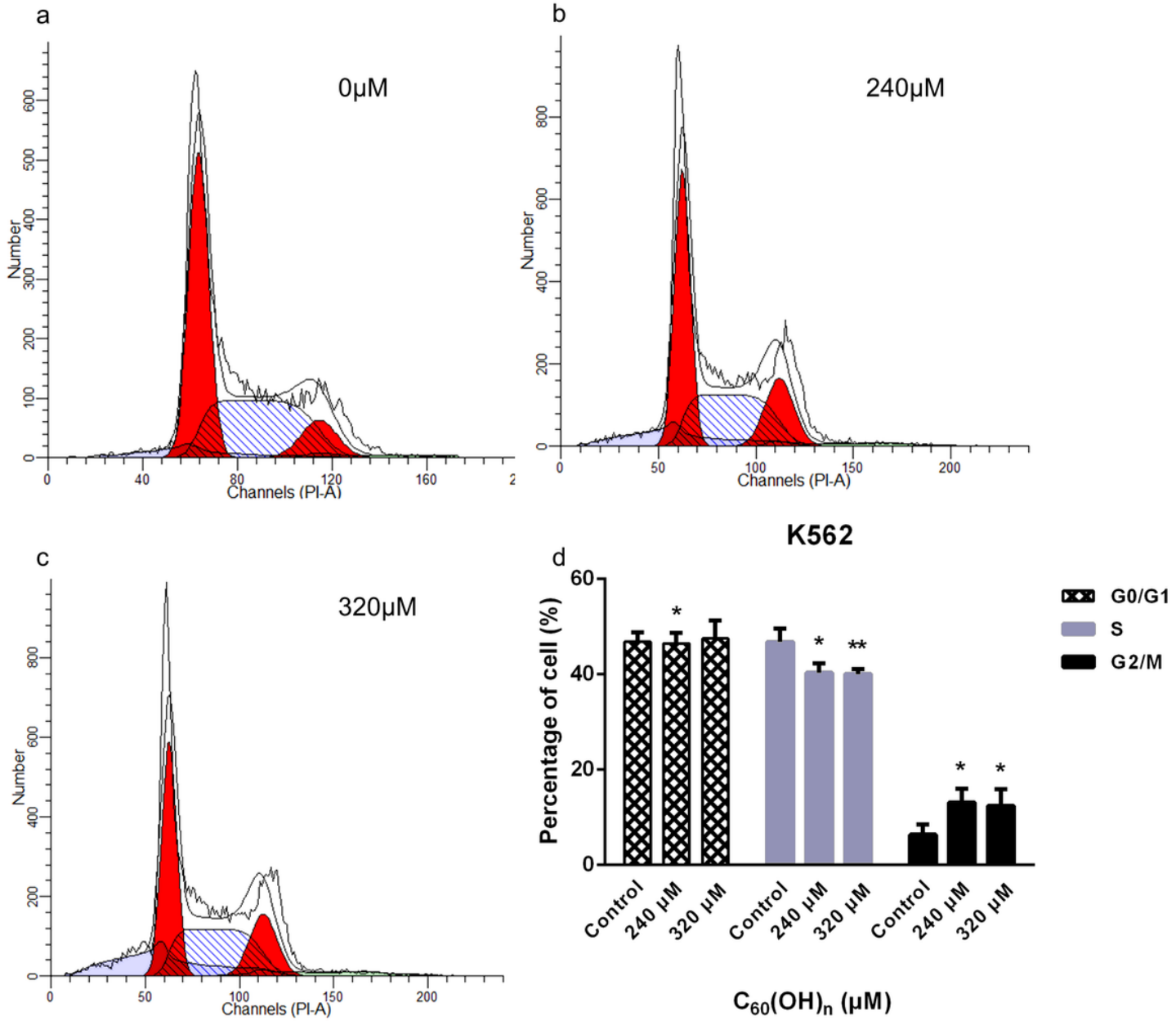

Figure 3

K562 cell cycle distribution. Following treatment with C60(OH)n for 48h, K562 cells were fixed and stained with the PI solution. The first peak in the graph was G0/G1 stage, followed by a broad peak representing the S stage, and the last peak was the G2/M phase. The data are expressed as the mean ± SD of at least three independent experiments. *P < 0.05 and **P < 0.01

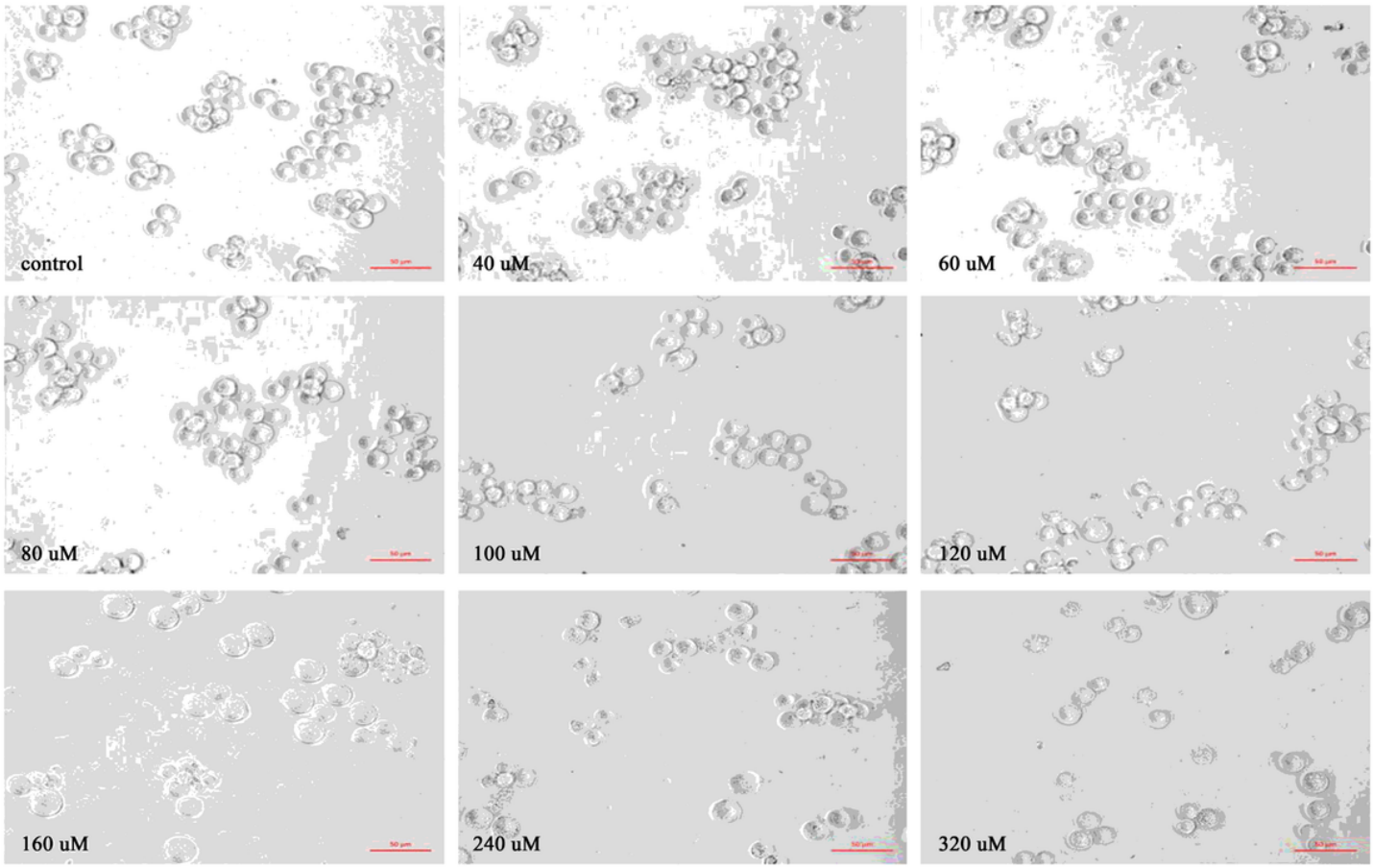

Figure 4

Influence of C60(OH)n on morphological characteristic and number of human chronic myeloid leukemogenic cells K562 incubated in vitro. Morphologic changes of unstained cells caused by C60(OH)n were measured using a fluorescence microscope (200×). Scale bars=50 μm. C60(OH)n at a dosage of 40, 60, 80, 100, 120, 160, 240, 320μmol/L, respectively, was administered to K562 cells for 48 h. All images

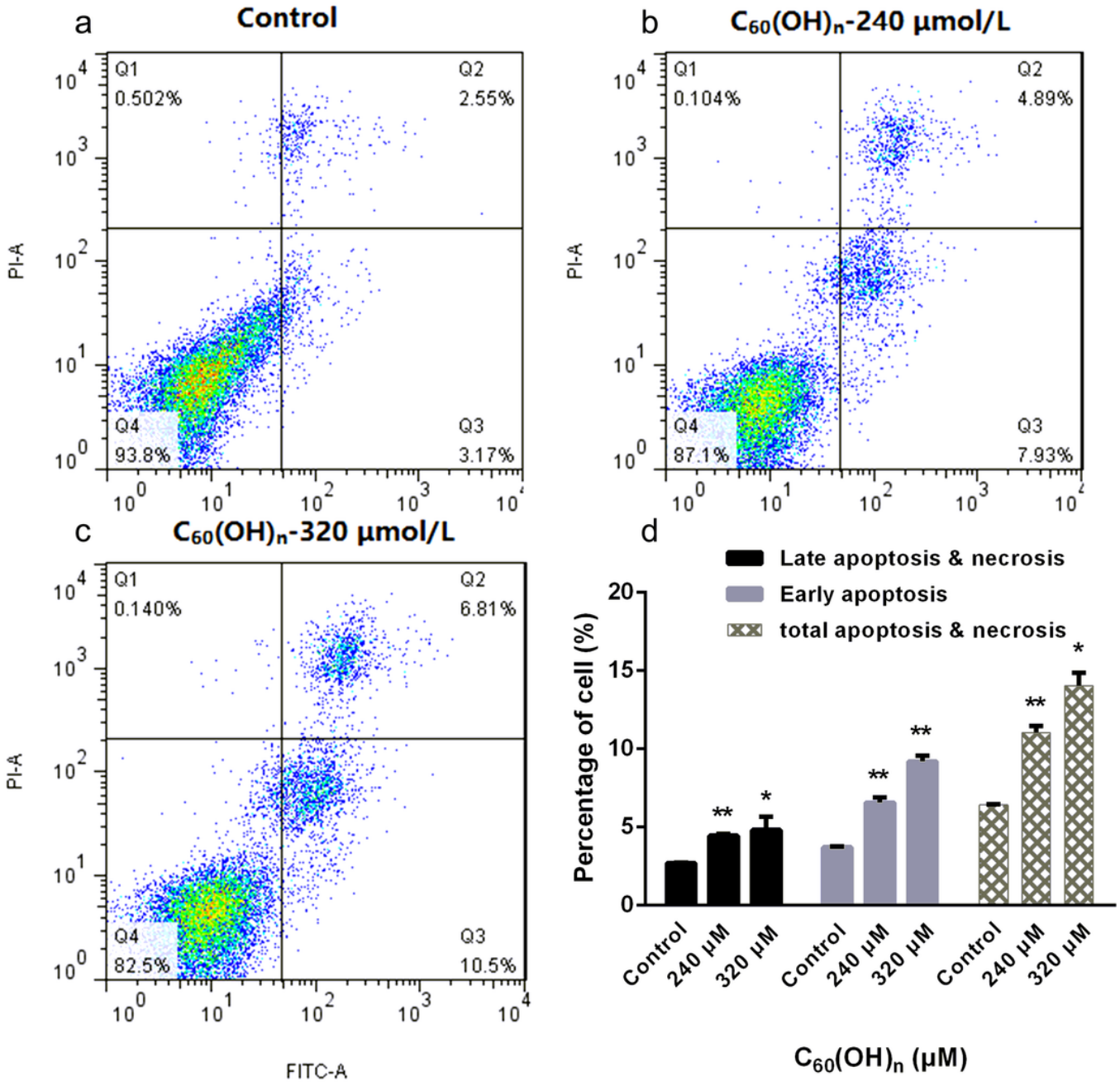

Figure 5

Effects of C60(OH)n on the induction of apoptosis. K562 cells were treated with C60(OH)n for 48h, and the apoptotic cell rate was analyzed using Annexin-V-FITC/PI staining. Data were presented as the mean ± SD of three independent experiments. *P < 0.05 and **P < 0.01

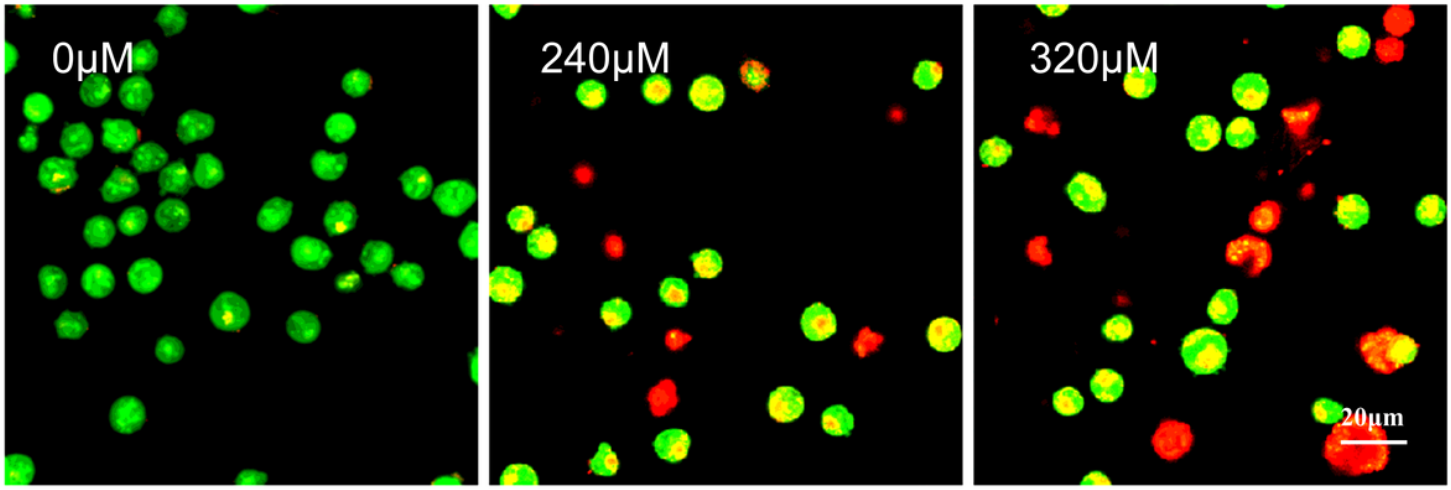

Figure 6

Representative images of nuclear condensation and DNA fragmentation in K562 cells exposed to C60(OH)n (600*). Nuclei were detected by AO/EB co-staining. All images shown were representative of three independent experiments

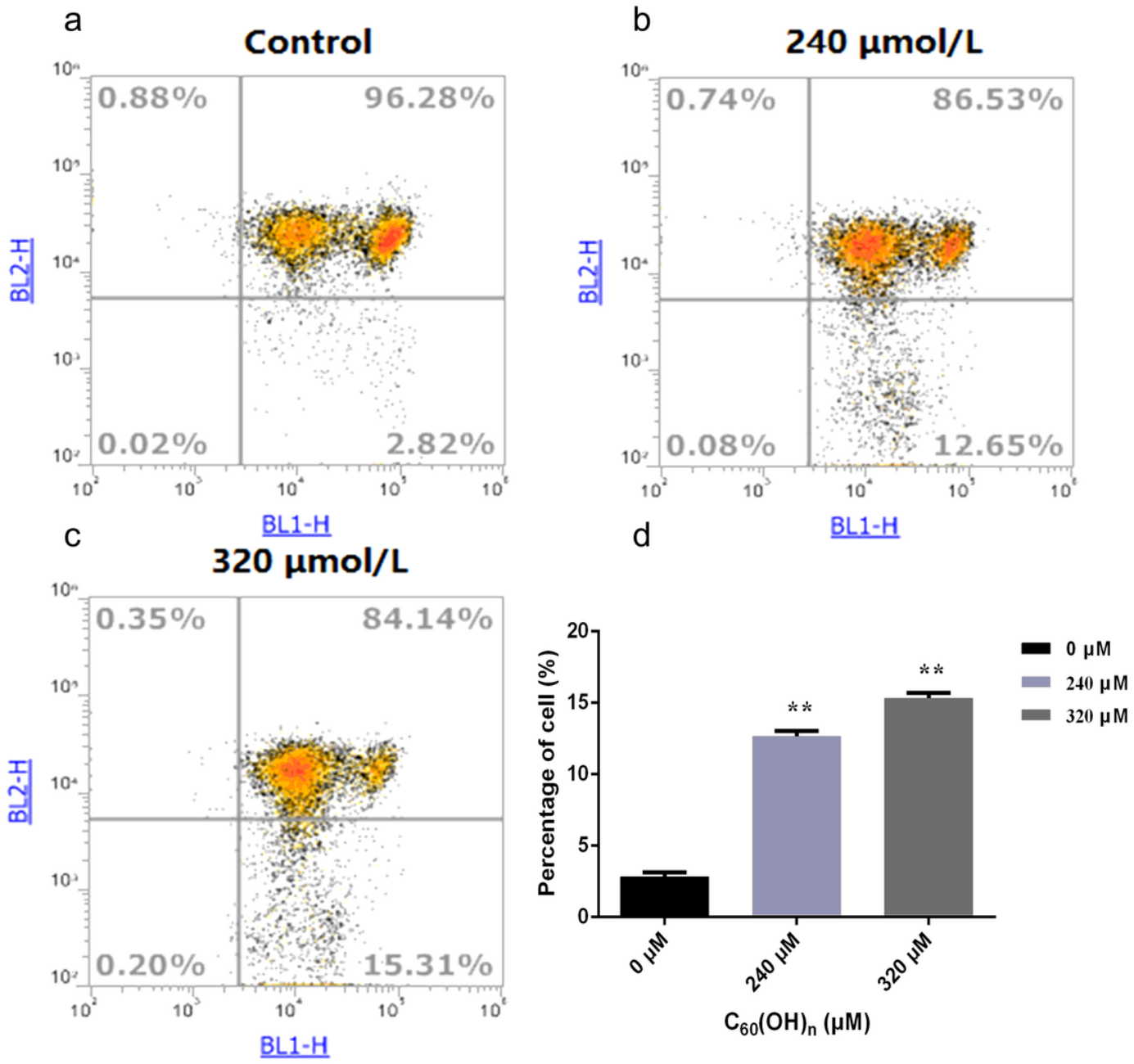

Figure 7

Flow cytometry analysis of MMP (ΔΨm) based on JC-1 staining. Cells were cultured with C60(OH)n for 48h and stained with JC-1.

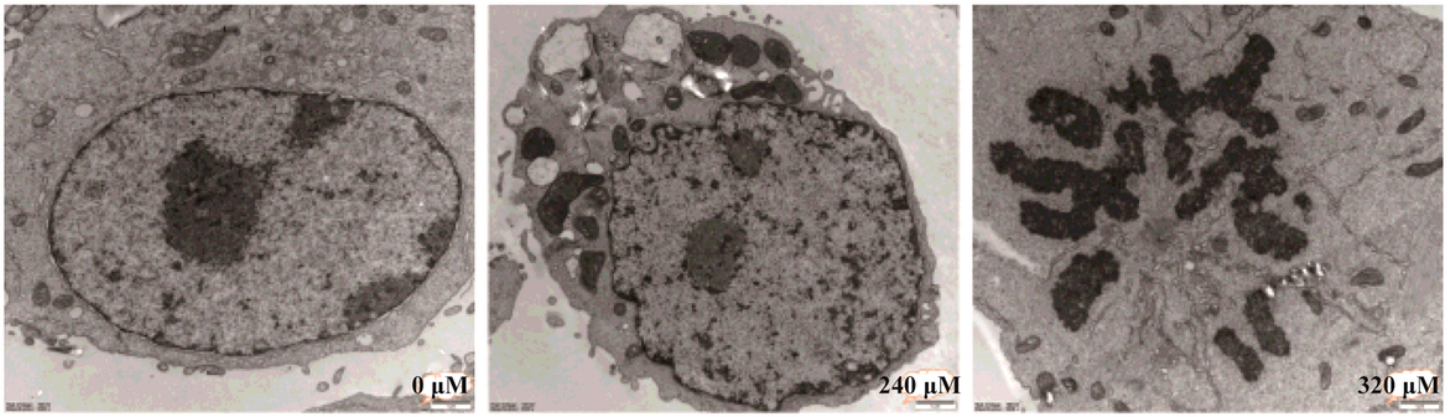

Figure 8

Observation of characteristic ultrastructural changes in K562 cell apoptosis after treatment with C60(OH)n(n=18-22). The ultrastructure of the apoptosis in K562 cells following treatment with 240, 320μmol/L C60(OH)n for 48h, respectively, was observed under the electron microscope. All images shown were representative of three independent experiments that appeared similar results. Scale bars=1 μm.